



Synthesis of hydrogels based on nanocellulose from garlic straw and regulating the release of allicin and its cytotoxicity

Xudong GAO^{1,2}, Yanan JIA¹, Zhongqin CHEN¹, Ramesh Kumar SANTHANAM³, Min ZHANG⁴, Chengwei HE⁵, Haixia CHEN^{1*} 

Abstract

Allicin is an organosulfur compound found in garlic, which is well known for their anticancer properties, however, its application was limited due to its instability towards light, heat, and alkaline conditions. In order to improve the bioavailability and stability of allicin, allicin was loaded into the garlic straw nanocellulose hydrogels and its physiochemical properties and toxicity towards normal hepatocyte cells (L02) and cancerous cells (HepG2) were evaluated. Initially, garlic straw was used as raw material to extract cellulose (GSC) and the garlic straw nanocellulose (GSNC) with a particle size of 168.0 ± 0.65 nm was prepared. Then, GSNC hydrogels were further prepared. The swelling rate of hydrogels in various medium was also determined. Finally, allicin was loaded into the hydrogels. The results showed that GSNC hydrogels had the porous structure, high pH sensitivity and the swelling rate in simulated intestinal fluid was 3054.24%. The drug loading capacity of allicin was 166.4 mg/g and the entrapment efficiency of allicin in GSNC hydrogel was 83.20%. The release rate of allicin-GSNC hydrogel was the highest in simulated intestinal fluid, and it could release allicin slowly. Moreover, the allicin-GSNC hydrogel were non-toxic towards L02 cells and had obvious toxicity towards HepG2 cells.

Keywords: garlic straw; allicin; hydrogels; anticancer; drug release.

Practical Application: Garlic straw nanocellulose hydrogels could improve the bioavailability and stability of allicin.

1 Introduction

Allicin (Diallyltrisulfide) is a special constituent of sulfur compounds found in garlic. It is a complex of multiple sulfur compounds (Fufa, 2019). The main components are diallyl sulfide (DAS), diallyl disulfide (DADS), diallyl trisulfide (DATS) (Melguizo-Rodríguez et al., 2022). It has significant cell inhibition and apoptosis promoting effect towards a variety of tumor cells (Schultz et al., 2020; Rosas-González et al., 2020; Salehi et al., 2019; Shang et al., 2019). The mechanism of action of allicin towards the cancerous cells are inhibition of cell proliferation and growth, induction of apoptosis, and prevention of angiogenesis, invasion and migration (Batiha et al., 2020). Though allicin has a wide range of pharmacological applications such as antibacterial, anticancer and antioxidant activities, due to their physiochemical nature such as low solubility in aqueous solution and their sensitivity towards light, heat and alkaline conditions (Salehi et al., 2019) as well as irritation in human mucous membranes and low bioavailability, the utilization of allicin in various medicinal applications are still limited. Studies suggested that the bioavailability of allicin could be utilized *via* encapsulating it with many drug delivery systems, such as microcapsules (Wang et al., 2018), liposomes (Lu et al., 2014) or nanoparticles (Soumya et al., 2018).

Hydrogel is a hydrophilic three-dimensional polymer network prepared by mixing cross linked polymers with water or other biological fluids. It has the capacity to swell in water and it undergoes a gel-sol phase transition in response to certain physical and chemical inducements (Yi et al., 2021). Hydrogels have wider application in the field of drug release (Lou et al., 2020; Xie et al., 2021; Zhang et al., 2020). The polymers used to prepare hydrogels can be obtained from synthetic or natural sources. In terms of pharmaceutical applications many researchers preferred to use the polymers from natural sources such as alginate, chitosan, cellulose, dextran, guar gum, hyaluronic acid okra gum, pullulan, xanthan etc. in the preparation of hydrogels as they could easily adhere to the biomembrane, penetrate into the mucus layers and get digested *in vivo*. Moreover it is non-toxic (Hanafy et al., 2020).

Cellulose is a kind of abundant natural polymer and its main structural unit is β -D-glucopyranosyl, where it linked with each other through 1, 4- β glycoside bond and it leads to form a linear polymer (Dai et al., 2019b). It has several advantages such as good biocompatibility, biodegradability, environmental friendliness and non-toxicity (Thakur & Thakur, 2014). Nanocellulose is a modified form of cellulose with

Received 28 Apr., 2022

Accepted 16 June, 2022

¹Tianjin Key Laboratory for Modern Drug Delivery & High-Efficiency, School of Pharmaceutical Science and Technology, Tianjin University, Tianjin, P. R. China

²General Hospital of Northern Theater Command, Shenyang, P. R. China

³Faculty of Science and Marine Environment, Universiti Malaysia Terengganu, Kuala Nerus, Terengganu, Malaysia

⁴College of Food Engineering and Biotechnology, Tianjin University of Science and Technology, Tianjin, P. R. China

⁵State Key Laboratory of Quality Research in Chinese Medicine, Institute of Chinese Medical Sciences, University of Macau, Taipa, Macao, P. R. China

*Corresponding author: chenhx@tju.edu.cn

nanostructures that has high strength, high crystallinity, high transparency and strong hydrophilicity (Kargarzadeh et al., 2017). The surface of nanocellulose contains a large number of hydroxyl groups, which further form the network structure through the hydrogen bond between the hydroxyl groups and their structural existence is very stable (Dias et al., 2021; Thakur et al., 2021). Thus, nanocellulose are widely used in the pharmaceutical field as biomaterials (Kamel et al., 2020; Nicu et al., 2021).

Garlic has a long history of use as a plant for both medicine and food. It has been found to be beneficial in adjuvant treatment of tumors, heart diseases, metabolic diseases, anti-inflammatory and anti-bacterial (Arslaner, 2020; Liu et al., 2022). It has been developed into a variety of products, such as Laba garlic, black garlic, etc (Lishianawati et al., 2022; Setiyoningrum et al., 2021; Gao et al., 2019a). But in garlic planting industry, mostly garlic straws are considered as waste, only a small part was used as fodder and most were burnt (Kallel et al., 2016). In this study, garlic straw as one of the wastes in garlic food processing industry was comprehensively utilized. It was conducive to guide the transformation of agricultural waste resources to green and high output value, which could not only improve economic benefits, but also effectively solve the environmental pollution caused by it. It was of great significance to the efficient utilization of food industry waste resources. The extracted cellulose (GSC) was converted to nanocellulose (GSNC) and further processed to form hydrogels (GSNC hydrogels). Fourier-transformed infrared spectroscopy (FTIR), scanning electron microscopy (SEM), X-ray diffractometer (XRD), texture profile analysis (TPA) and *in vitro* release techniques were used to evaluate the properties of the hydrogels. Then the compound, allicin was loaded into the hydrogels and their bioavailability, entrapment efficiency and drug loading capacity were evaluated. Additionally, the cytotoxicity of allicin, hydrogels and allicin loaded hydrogels were evaluated against normal hepatocyte L02 cells and cancerous cells (HepG2).

2 Materials and methods

2.1 Materials and chemicals

Garlic straw was purchased from the market (Shandong, China); Allicin (SA8721, HPLC grade), Pepsin (2500 U/mg), Trypsin (1500 U/mg) 3-(4, 43 5-dimethylthiazol-2-yl)-2, 5-diphenyltetrazolium bromide (MTT), Acrylamide (AM, purity $\geq 98.0\%$) and Methylene-Bis-Acrylamide (MBA, purity $\geq 99.0\%$) were purchased from Beijing Solarbio Science & Technology Co., Ltd. (Beijing, China); Sodium Chlorite (NaClO_2), Sodium Hydroxide (NaOH) and Acrylic acid (AA, purity $\geq 99.0\%$) were obtained from Adamas beta Reagent Co., Ltd (Shanghai, China); DMEM and fetal bovine serum (FBS) were obtained from Biological Industries Ltd. IATI (Israel Advanced Technology Industries). Penicillin-streptomycin solution was purchased from HyClone Co. (Utah, USA). All other chemicals and reagents were purchased locally and were analytical grade.

2.2 Extraction of cellulose and nanocellulose from garlic straw

Preparation of garlic straw cellulose

Garlic straw cellulose (GSC) was extracted according to the method by Dai and Huang with minor modifications (Dai & Huang, 2016). The garlic straw was crushed by a pulverizer and passed through a 100 mesh sieve. Then 100 g of garlic straw powder was soaked in 2 L of deionized water at 80 °C for 2 h to remove the water-soluble components. The garlic straw powder filter residues were washed repeatedly with deionized water to clarify and the residues were dried at 50 °C overnight. Next, 1.2 L of 7.5% NaClO_2 solution (adjust pH value to 4.0 with HCl solution) was added and kept in water bath at 75 °C for 2 h to remove lignin and bleach the filter residues. Further, filtered and washed the residues with deionized water to neutral. Then washed residues with 95% ethanol, dried them at 50 °C overnight. The residues were treated with 1.2 L of 10% NaOH solution in a shaker at room temperature for 12 h and then ultra-sonicated thrice for 20 min to remove hemicellulose and impurities. The residues were finally washed with deionized water for neutralization, then washed them with 95% ethanol for dehydration and freeze-dried. 17.9 g of GSC was obtained.

Preparation of garlic straw nanocellulose

Garlic straw nanocellulose (GSNC) was prepared according to Dai et al. with few modifications (Dai et al., 2019a). Briefly, all GSC obtained in the previous step were treated with 30% H_2SO_4 , and then H_2SO_4 was added drop by drop and the mixture was continuously mechanically stirred (500 rpm) until the final concentration of concentrated sulfuric acid reached 60%. Next it was sonicated (600 w) for 15 min and repeated 3 times. Then, the reaction was terminated with 10 times the volume of anhydrous ethanol to obtain white flocculent precipitate, washed them with deionized water to pH 7.0, and subjected to freeze-dry. 14.56 g of garlic straw nanocellulose (GSNC) was obtained.

2.3 Prepared the GSNC hydrogels

Initially, 4 g of GSNC was mixed with 100 mL of deionized water at room temperature and stirred until completely dispersed; the solution was heated to 60 °C and purged with N_2 for 30 min, then 0.1 g of APS (Ammonium Persulfate) as the initiator was added to GSNC solution, stirred at 60 °C for 15 min and then 20 mL of AA (Acrylic acid, 70% neutralization degree), 4 g of AM (Acrylamide) and 0.12 g of MBA (Methylene-Bis-Acrylamide) was added to the solution, respectively. The whole reaction should be carried out in N_2 atmosphere, subsequently, the mixture was stirred at 70 °C for 10 min to obtain GSNC hydrogels. After the GSNC hydrogels was cooled to room temperature, the residual unreacted compounds were removed with 10% NaOH solution and deionized water respectively and washed to pH 7.0, and then the GSNC hydrogels were obtained.

2.4 Characterization of GSC, GSNC and GSNC hydrogels

Zeta potential of GSNC

The GSNC sample was diluted 10 times in deionized water with a total volume of 1 mL, and then the particle size was analyzed at 25 °C. The particle size of GSNC was determined using laser particle size analyzer (Malvern Zetasizer Nano ZS90, Malvern Instruments, U.K.).

FTIR spectroscopic analysis

Agate mortar was used for freeze-dried samples of GSC, GSNC and GSNC hydrogels ($\Phi = 60$) crushed and pass the 100 mesh sieve, then they were mixed with 100-200 mg of dried KBr powder, respectively. The FTIR spectrum data of each sample were recorded by KBr pressed pellet method using FTIR spectrometer (tensor 27, Bruker, Germany) measured at the resolution at 4 cm^{-1} from 4000 to 500 cm^{-1} (Ge et al., 2019).

Scanning Electron Microscope (SEM) microscopy

Freeze-dried the pre-swelling equilibrium GSNC hydrogels, then quenched them with liquid nitrogen and pasted them on the sample table with conducting resin and sprayed the samples with gold. SEM images of the samples were observed using a desktop scanning electron microscope (Phenom Pro, Phenom, Netherlands). The samples were imaged at an accelerating voltage of 15 kV.

X-ray Diffraction (XRD)

Each group of samples was crushed to powder and passed through 320 mesh sieve (about 40 μm) and weighed 3-5 g powder for test. X-ray diffractometer data (XtaLAB Synergy, Rigaku, Japan) was used to obtain XRD data of the samples by Cu K α radiation ($\lambda = 0.15406$ nm), the diffraction angle (2θ) was 4° to 40°, the scanning speed was 2°/min, and the voltage and current were 40 kV and 40 mA, respectively.

2.5 Determination of swelling properties of GSNC hydrogels

The swelling properties of GSNC hydrogels were evaluated according to the method described by Fattahpour et al. (2020). The freeze dried material of GSNC hydrogels was cut into pieces (1 cm \times 1 cm \times 1 cm) and the weight was recorded. Then the GSNC hydrogels were soaked in distilled water, simulate intestinal fluid (SIF), simulate gastric fluid (SGF) and buffer solution (pH 5.5) at 25 °C. The GSNC hydrogels were removed at intervals of 1 h, and the excess surface liquid was removed with the filter paper, then the mass of GSNC hydrogels was recorded accurately. The equilibrium swelling rate (ESR) of hydrogels was calculated according to the Equation 1:

$$ESR(\%) = \frac{W_s - W_d}{W_d} \times 100 \quad (1)$$

Where W_s (g) is the weight of swollen hydrogels, W_d (g) is the weight of dried hydrogels.

2.6 GSNC hydrogels Texture Profile Analysis (TPA)

Mechanical properties of GSNC hydrogels were determined by the method in the literature (Yan et al., 2020). The GSNC hydrogels was cut into 1.5 cm^3 cube-shaped samples, and its hardness, elasticity, cohesiveness, gumminess, stickiness and recovery were measured using a texture analyzer (TA XT plus, Stable Micro System, UK). Before measurement, the GSNC hydrogels were soaked in deionized water for 48 h at 25 °C and then the texture profile analysis (TPA) of GSNC hydrogels was performed at room temperature using the TA XT plus texture analyzer with a P/36R stainless steel probe at a test speed of 1 mm/s. Mechanical properties were measured in three replications.

2.7 Drug loading of allicin on GSNC hydrogels

The preparation of allicin-GSNC hydrogels sample was done by the method described by Dai et al. with minor modifications (Dai et al., 2019a). In this study, 50 mg of dried GSNC hydrogels were immersed in 10 mL allicin solution (1 mg/mL, dissolved in 30% ethanol solution) at 25 °C for 24 h. The GSNC hydrogels were removed from the allicin solution and rinsed 3 times with the 30% ethanol solution to remove free allicin and the loaded hydrogels were freeze-dried for further study. The drug loading content (DL) and encapsulation efficiency (EE) were calculated according to the Equations 2 and 3, respectively.

$$DL(\text{mg/g}) = \frac{M_T - M_F}{M_H} \quad (2)$$

$$EE(\%) = \frac{M_T - M_F}{M_T} \times 100 \quad (3)$$

Where M_T is the total weight of allicin, M_F is the weight of free allicin, and M_H is the weight of GSNC hydrogels.

2.8 In vitro drug release

Simulated gastric fluid (SGF), simulated intestinal fluid (SIF) and PBS buffer (pH5.5) was prepared. Initially, 1.64 mL of HCl was added to 80 mL of deionized water and then 1 g of pepsin was mixed and diluted to 100 mL with deionized water to obtain SGF. For SIF, 0.68 g of potassium dihydrogen phosphate (KH_2PO_4) was dissolved in 50 mL of distilled water, and the pH value was adjusted to 6.8 with 0.1 M NaOH solution, then 1 g of trypsin was added, mixed well, and diluted to 100 mL with distilled water. The release study of allicin from GSNC hydrogels was performed at 37 °C in different medium (SGF, SIF and pH 5.5 of PBS) using diffusion technique (Eftaiha et al., 2010). Allicin-GSNC hydrogels (5 mL, 1 mg/mL) solution was added into the dialysis bag (molecular weight cut off 3500 Da) and immersed in 50 mL medium (SGF, SIF or pH 5.5 of PBS) and the whole set up was continuously stirred at a rotating speed of 100 rpm. At regular intervals, 200 μL of the medium was removed and replaced with the same amount of fresh medium. The amount of released drug was determined using UV-Visible spectroscopy at 210 nm. The drug release (DR) percentage was calculated using following Equation 4:

$$DR(\%) = \frac{M_t}{M_0} \times 100 \quad (4)$$

Where, M_t and M_0 represent the amount of released and loaded drug with time, t , respectively.

2.9 Cell culture and cytotoxicity assay

The cytotoxic effects of allicin, GSNC hydrogels and allicin-GSNC hydrogels in HepG2 cells and L02 cells were evaluated using MTT assay (Gao et al., 2019b). HepG2 cells and L02 cells were obtained from the Cell Resource Center of the Shanghai Academy of Sciences (Chinese Academy of Sciences, China). Briefly, cells were cultured in DMEM medium with 10.0% FBS, 1% penicillin-streptomycin at 37 °C in 5% CO₂ atmosphere. Cells were seeded in the 96-well plates at the density of 1×10^4 cells/well. Once the cells reached more than 80% confluence, a series of concentration (10-1000 µg/mL) of samples were added to the cells. All the samples were dissolved in fresh DMEM media with 0.05% DMSO. After 24.0 h, 20 µL MTT solution (5.0 mg/mL, dissolved in PBS) was added to each well and incubated at 37 °C for 4 h. Then the supernatant was removed and 180 µL of DMSO was added to each well. The absorbance reading was measured at 490 nm using microplate reader (Tecan Infinite Pro, M1000, Switzerland).

2.10 Statistical analysis

All the data were represented as Mean \pm SD. Data analysis were performed using one way ANOVA followed by Dunnett test in Graphpad prism software (Version 5). $P < 0.05$ was considered to be statistically significant.

3 Results and discussion

3.1 Particle size and zeta potential of GSNC

The diameter and poly dispersity index (PDI) of GSNC were measured using DLS mode at 25 °C *via* proper dilutions. As shown in Figure 1, the average particle size of GSNC dispersed in deionized water at 25 °C was 168.0 ± 0.65 nm, and the PDI value was 0.358 ± 0.10 nm. PDI is an indicator of the particle size distribution, and the value < 0.4 represents the particle possess narrow distribution which is better for uniformity. Two normal distribution peaks in the particle size distribution of GSNC were obtained, which indicated that the GSNC was an aspheric particle, and there were significant differences in particle sizes in different directions, which was consistent with the shape characteristics of cellulose. Overall, GSNC had small particle size, uniform morphology, and it could be used in preparation of *in vivo* and *in vitro* drug carriers.

3.2 Preparation process of GSNC hydrogels

The reaction process for preparing GSNC hydrogels was shown in Figure 2. GSNC as the reaction model, APS as reaction initiator, AA and AM as reaction monomer and MBA as reaction crosslinking agent, the polymerization was carried out by chemical initiation. Sulfate radicals were formed when APS was at the temperature of the reaction, and then acted on cellulose backbone to produce hydroxyl radicals. When AA and AM were added, the free radicals formed in cellulose backbone could attack C=C in AM and connect with it to achieve chain

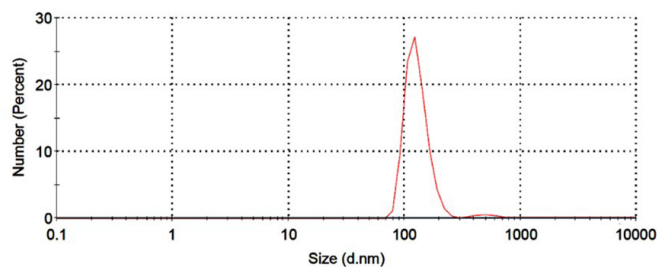


Figure 1. The particle size distribution of Garlic Straw Nanocellulose (GSNC).

growth. During the chain growth, the terminal vinyl group of MBA reacted with various polymer chains, and finally a cross-linked structure was synthesized.

3.3 FTIR analysis of GSC, GSNC and GSNC hydrogels

The FTIR spectra of GSC, GSNC and GSNC hydrogels were shown in Figure 3. The broad peaks observed at the region of 3000 to 3600 cm⁻¹ were the stretching vibration absorption peaks of -OH (Nasef et al., 2019). The broad band between 3410 cm⁻¹ and 2900 cm⁻¹ were the characteristic peaks of cellulose, mainly formed by hydrogen bonds, the absorption peak at 2901 cm⁻¹ was related to the stretching vibration peak of -CH in methyl, methylene and methane (Valentim et al., 2018); the peaks at 1427 cm⁻¹ and 1369 cm⁻¹ corresponded to the bending vibration of -CH₂ (Hosseinzadeh et al., 2019). The peak of 1161 cm⁻¹ was the asymmetric stretching vibration of resonance C-O-C in cellulose; the peak of 1064 cm⁻¹ was the stretching vibration of C-O group and the β-D glucoside bond in the sample was characterized at 900 cm⁻¹, these data were consistent with the study of Abidi et al. (2014). In the GSNC hydrogels, the characteristic peak near 900 cm⁻¹ disappeared, indicating that the β-D glucoside bond between the glucose units of cellulose disappeared; the peaks at 3638 cm⁻¹ and 1050 cm⁻¹ were -OH stretching vibration and C=O stretching vibration; the O-H out of plane (OOP) vibrations appeared at 612 cm⁻¹, the peaks at 1651 cm⁻¹ and 1550 cm⁻¹ belonged to the amide I band (The stretching vibration of C=O in CONH₂ group) and the absorption peak of amide II band (the bending vibration of N-H in CO-NH) (Anirudhan & Rejeena, 2014; Huang & Shen, 2014), the results implying that the GSNC was grafted successfully with AM and MBA.

3.4 Crystalline structure of GSC, GSNC and GSNC hydrogels

XRD technique was used to characterize the crystallinity of the polymer. The XRD patterns of GSC, GSNC and GSNC hydrogels were compared in Figure 4. As shown in Figure 4, the XRD data of GSC displayed three diffraction peaks at $2\theta = 16.49^\circ$, 22.5° and 34.48° which corresponded to the (101), (002) and (040) crystal planes, respectively, which belonged to cellulose type I (Yan et al., 2020). In addition, GSC had a strong diffraction peak at $2\theta = 24.67^\circ$, which was the characteristic peak of hemicellulose, which might be due to cellulose containing hemicellulose (Li et al., 2018).

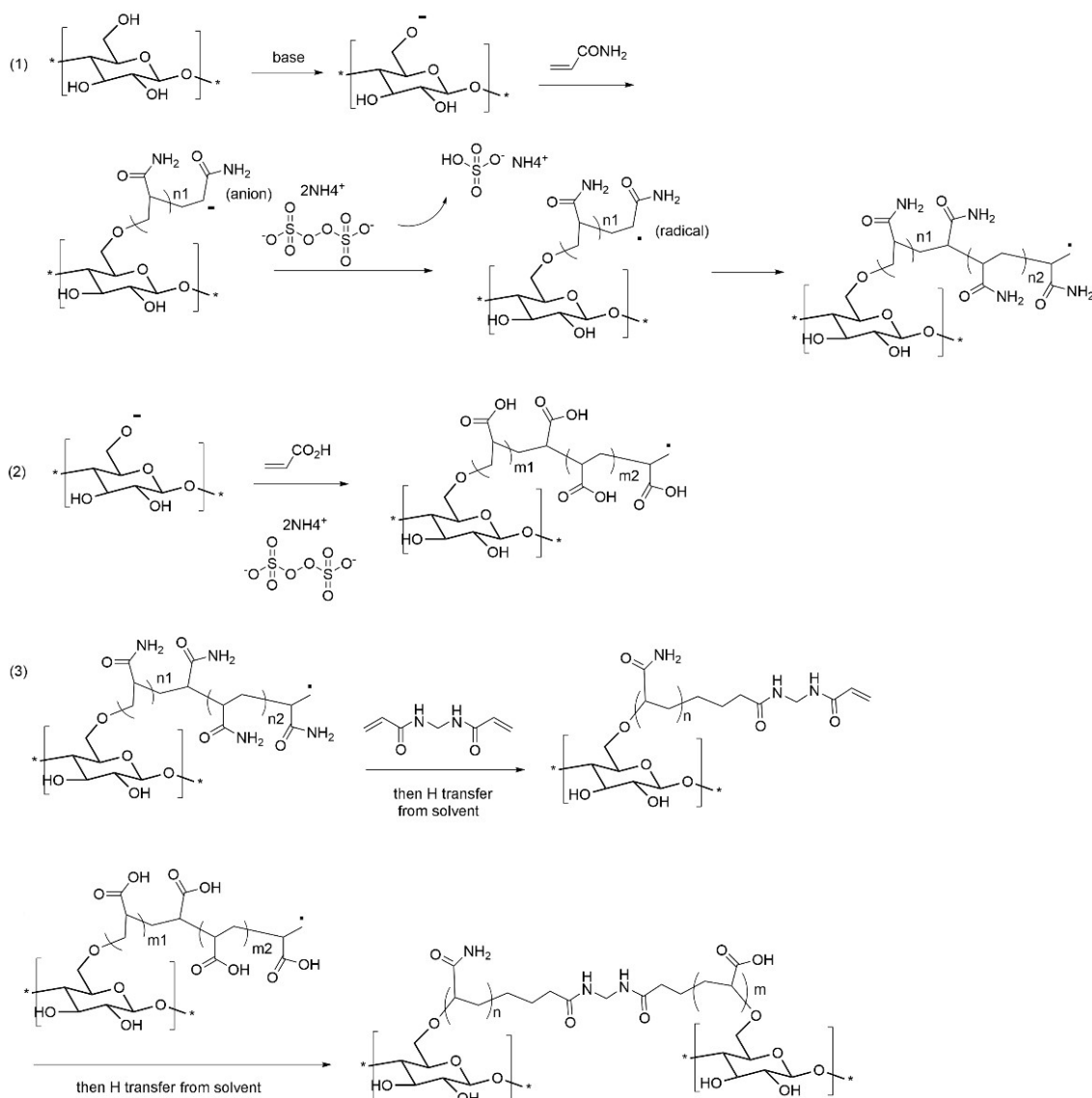


Figure 2. Mechanism of Garlic Straw Nanocellulose (GSNC) hydrogels formation. (1) The initiator APS was heated to decompose into sulfate anion radical, and then captured a hydrogen atom from the hydroxyl group of GSNC chain to form Cellulose-O \cdot , and acrylamide was further added to realize the extension of GSNC chain; (2) Acrylic acid was further added to realize the extension of GSNC chain; (3) During the chain extension period, the terminal vinyl of the crosslinking agent MBA reacts with the above two polymers to obtain a crosslinked structure (GSNC hydrogels).

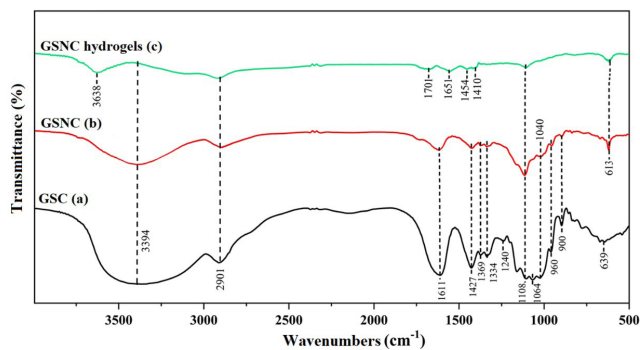


Figure 3. FTIR spectrum of Garlic Straw Cellulose (GSC) (a), Garlic Straw Nanocellulose (GSNC) (b) and GSNC hydrogels (c).

The XRD pattern of GSNC showed four peaks at $2\theta = 12.01^\circ$, 19.90° , 20.30° and 21.89° , which indicated a cellulose type II crystalline structure (Dai & Huang, 2016). In addition, GSNC also had diffraction peaks at $2\theta = 16.49^\circ$, 22.5° and 34.48° , but the peak height was significantly lower than that of GSC. The results showed that during the process of preparing nanocellulose, the crystal structures of cellulose have been changed, and cellulose type I and type II coexisted in GSC. Moreover, there was a characteristic peak at $2\theta = 25.65^\circ$, which indicated that a six-membered carbon ring structure existed in GSNC (Cheng et al., 2019). It was proved that the crystal structure of GSC was destroyed and the crystal planes changed significantly during the processing of GSC into GSNC.

In GSNC hydrogels, there were three diffraction peaks at $2\theta = 12.50^\circ$, 19.90° and 20.50° , which belonged to cellulose type II, and there were two weak diffraction peaks at $2\theta = 14.78^\circ$ and 16.49° , which belonged to cellulose type I; a strong diffraction peak appeared at $2\theta = 32.5^\circ$, and the diffraction peak disappeared at $2\theta = 22.50^\circ$, which might be due to the hydrogen bonding

interaction between AM and MBA and GSNC. The grafting of AM and MBA with GSNC destroyed the intermolecular hydrogen bonding in GSNC.

3.5 Morphological analysis of GSC, GSNC and GSNC hydrogels

Figure 5a-5c are the macroscopic morphologies of GSC, GSNC, and GSNC hydrogels, respectively. GSC was the white short stick-like powder, and GSNC was the freshly prepared nanocellulose with the white colloidal shape. Figure 5d-5f are SEM micrographs of GSC, GSNC and GSNC hydrogels, respectively. Due to the removal of part of lignin and hemicellulose, the surface of GSC was smooth and has the appearance of sheet structure (Figure 5d) (Yan et al., 2020). As shown in Figure 5e, GSNC was filamentous shape with the large particle size, which might be due to agglomeration of GSNC after freeze-dried. From Figure 5f, the porous structure of GSNC hydrogels could be observed. The results showed that this porous structure was responsible for carrying water and showed good drug loading capacity. Based on this rough and fluffy structure, the good swelling capacity was observed (Figure 5g-5h). Many studies have shown that porous hydrogels were beneficial for swelling, drug loading and drug release.

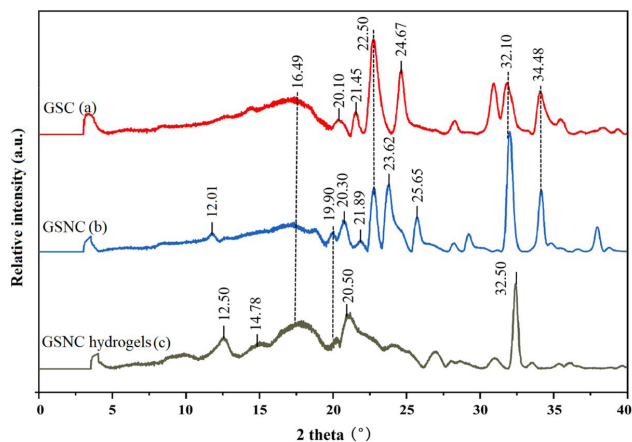


Figure 4. XRD patterns of Garlic Straw Cellulose (GSC) (a), Garlic Straw Nanocellulose (GSNC) (b) and GSNC hydrogels (c).

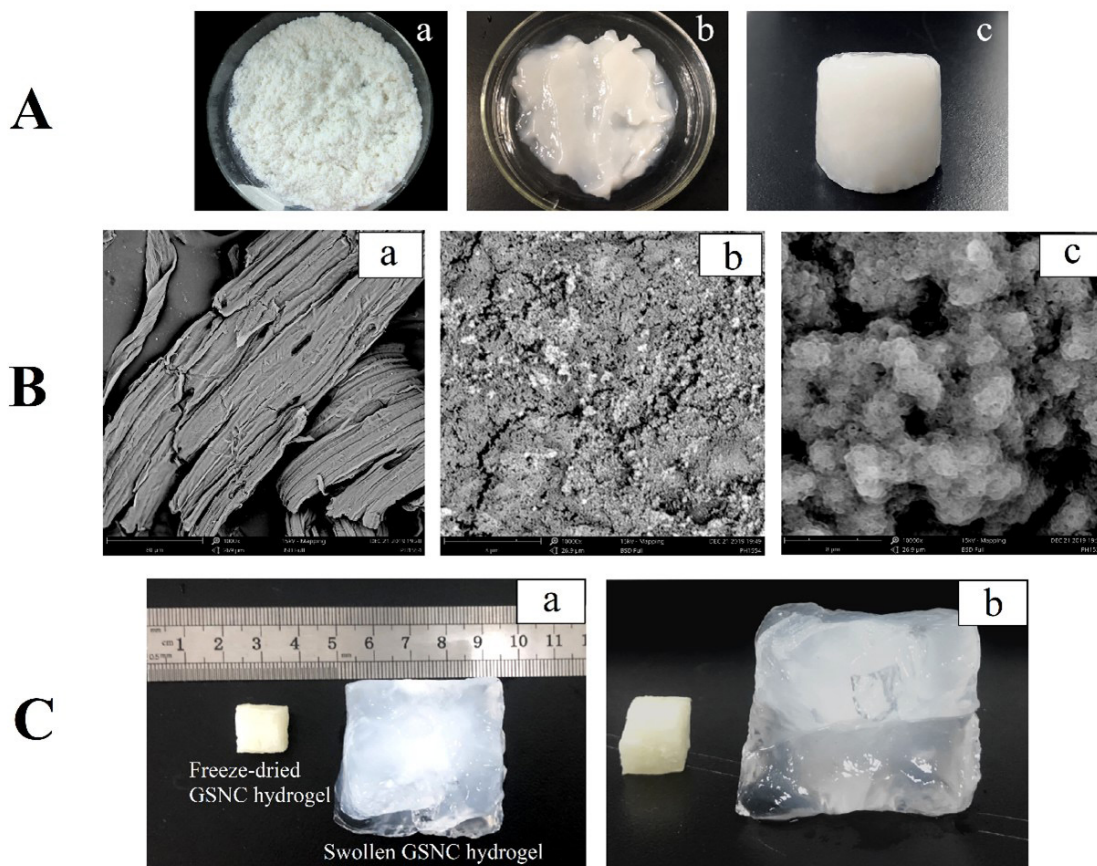


Figure 5. Morphology observation of Garlic Straw Cellulose (GSC), Garlic Straw Nanocellulose (GSNC) and GSNC hydrogels. (A) The macroscopic morphology of GSC (a), GSNC (b), GSNC hydrogels (c); (B) SEM images (10000 \times) of GSC (a), GSNC (b) and GSNC hydrogels (c); (C) Swelling of GSNC hydrogels (a & b).

3.6 Swelling studies of GSNC hydrogels

The swelling behavior of GSNC hydrogels was observed in various mediums, and the pH values of various mediums were different (SGF, SIF, pH 5.5 of PBS and distilled water), which confirmed that GSNC hydrogels were responsive/sensitive to pH (Figure 6). As shown in Figure 6, GSNC hydrogels could swell in various mediums within 0-24 h. Within 24 h, GSNC hydrogels had the best swelling performance in SIF, and the ESR_{Max} value was 3054.24%. In distilled water, PBS (pH 5.5), and SGF were 2922.45%, 2499.79%, and 1175.43%, respectively. The results proved that the sensitivity of GSNC hydrogels was different in various pH values mediums. This might be due to the -COOH in AA, the effects of intermolecular hydrogen bond and hydrophobic bond limited the swelling of GSNC hydrogels, leading to the swelling rate of GSNC hydrogels was decreased (Gharekhani et al., 2017). In contrast, in weakly alkaline medium, the increase in the swelling rate of GSNC hydrogels was due to the enhanced electrostatic repulsion of COO⁻, the repulsion between the same charges was stronger than the attraction between different charges, which led to the outward expansion of the hydrogels network (Dai et al., 2019a). Therefore, GSNC hydrogels had good pH sensitivity. Under weak alkaline conditions, the swelling rate was high and the swelling equilibrium was quickly reached, which was beneficial to the rapid absorption of drugs in the intestine.

3.7 Mechanical properties of GSNC hydrogels

The textural parameters of GSNC hydrogels were determined by TPA. The results were shown in Table 1. The results showed that the springiness of GSNC hydrogels was close to 1, indicated that it was highly elastic, GSNC hydrogels had good mechanical properties. Compared with the mechanical properties of the hydrogels prepared by celery cellulose studied by Yan et al. (2020), the data of hardness/g, gumminess, springiness, cohesiveness

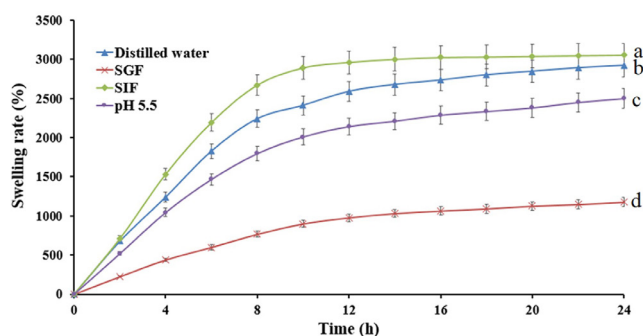


Figure 6. Swelling behavior of the Garlic Straw Nanocellulose (GSNC) hydrogels. Data are expressed as mean \pm SD ($n = 3$). Different small letters indicate a significant difference ($P < 0.05$).

Table 1. The mechanical properties of GSNC hydrogels in TPA test.

Sample	Hardness/g	Springiness	Cohesiveness	Gumminess	Resilience
GSNC hydrogels	4449.275 \pm 23.230	0.926 \pm 0.107	1.012 \pm 0.190	3625.358 \pm 12.980	0.692 \pm 0.101

The values represent means of triplicate \pm SD.

and resilience of GSNC hydrogels were several to dozens times of that of celery cellulose hydrogels. The outstanding mechanical properties of GSNC hydrogels were related to GSNC. Many studies have shown that compared with cellulose, nanocellulose has higher mechanical strength, higher young's modulus and stronger hydrophilicity. Therefore, nanocellulose could be used as a biochemical material with great development potential.

3.8 Drug loading and encapsulation efficiency of GSNC hydrogels

The drug loading content and the entrapment efficiency of allicin into the GSNC hydrogels were determined using ultracentrifugation technique, and the percentage of entrapment was determined using the UV absorption method. The drug loading content and the percentage of entrapment efficiency of allicin-GSNC hydrogels were 166.40 mg/g and 83.20%, respectively. GSNC hydrogels had high drug loading capacity and better encapsulation capacity for allicin, which was closely related to the porous structures.

3.9 In vitro release studies

In order to evaluate the potential application of the drug delivery system, the release characteristics of allicin in the GSNC hydrogels were studied and the results were shown in Figure 7. The drug release of allicin and allicin-GSNC hydrogels in SGF, SIF and PBS (pH = 5.5) was detected by diffusion method (Figure 7). As shown in Figure 7A, the release rate of allicin was highest at pH 5.5 and that was lower in SIF, the release of drugs in hydrogels was basically composed of two stages, including the initial stage of a large outbreak and the subsequent slow release stage (Nounou et al., 2006). After 5 h, the release curve of allicin significantly decreased, which might be due to the degradation of allicin in the mediums.

From the release curve of the allicin GSNC hydrogels (Figure 7B), it could be seen that the allicin had a significant sustained release effect and the stability of allicin has been improved. The release rate of allicin-GSNC hydrogels after 30 h was the highest in SIF. The release rate of allicin-GSNC hydrogels in SIF was $83.8 \pm 1.22\%$ and tended to be stable after 120 h. The cumulative release rate in the simulated tumor environment (pH 5.5) was $55.38 \pm 0.87\%$, and it still showed an upward trend. According to previous studies (Kim et al., 1992), drug release from hydrogels was mainly controlled by drug-hydrogels interactions, drug solubility, and hydrogels swelling capacity. It was observed that the release curve of the hydrogels was consistent with the swelling data, indicated a positive correlation between swelling and the release of allicin.

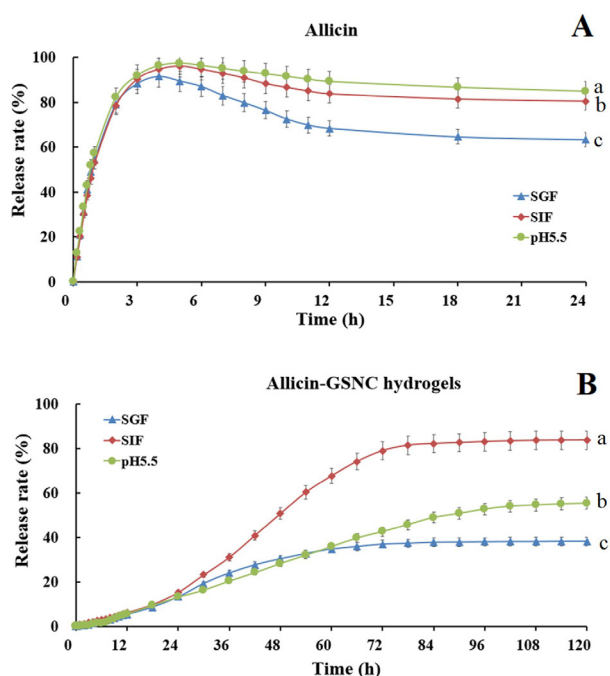


Figure 7. Release profiles *in vitro* of allicin (A) and allicin-Garlic Straw Nanocellulose (GSNC) hydrogels (B). All values are expressed mean \pm SD (n=3). Different small letters indicate a significant difference ($P < 0.05$).

3.10 Cytotoxicity evaluation of GSNC hydrogels

As a carrier, the biological material releases the drug into the human body and play an important role in pharmacology, thereby achieving the purpose of treatment. The interaction between materials and the human body could usually cause systemic reactions such as cellular reactions, tissue reactions, and blood reactions, resulting in serious hazards such as collective immunity and rejection (He et al., 2020; Qi et al., 2020). In this study, standard MTT method was used to detect the cytotoxicity of GSNC hydrogels and allicin-GSNC hydrogels (Gao et al., 2019b). The cytotoxic potential of allicin-GSNC hydrogels were determined against HepG2 cells and L02 cells. As shown in Figure 8A, allicin and allicin-GSNC hydrogels could significantly inhibit the growth of HepG2 cells. Among them, the maximum inhibition rate of allicin at 72 h was $91.54 \pm 0.81\%$, and the IC_{50} was $55.23 \pm 0.24 \mu\text{g/mL}$. The maximum inhibition rates of allicin-GSNC hydrogels at 24, 48 and 72 h were $42.37 \pm 0.54\%$, $82.31 \pm 1.01\%$ and $91.78 \pm 0.93\%$, respectively, and the IC_{50} were 133.56 ± 1.32 , 70.58 ± 0.39 and $52.30 \pm 0.22 \mu\text{g/mL}$. These results indicated that the GSNC hydrogels loaded with allicin in this study showed significantly inhibitory effect on HepG2 cells. Compared with the free allicin, the anticancer effect of the hydrogels was obviously released slowly. HepG2 cells were treated with allicin-GSNC hydrogels for 72 h, the IC_{50} value was lower than that of allicin group, indicated that the GSNC hydrogels could help the Allicin to enter the cell membrane and increase the bioavailability of allicin and it significantly enhance the inhibition on HepG2 cells proliferation. As shown in Figure 8B, all the samples were non-toxic to L02 cells within the concentration range of 10-1000 $\mu\text{g/mL}$. Therefore, it was

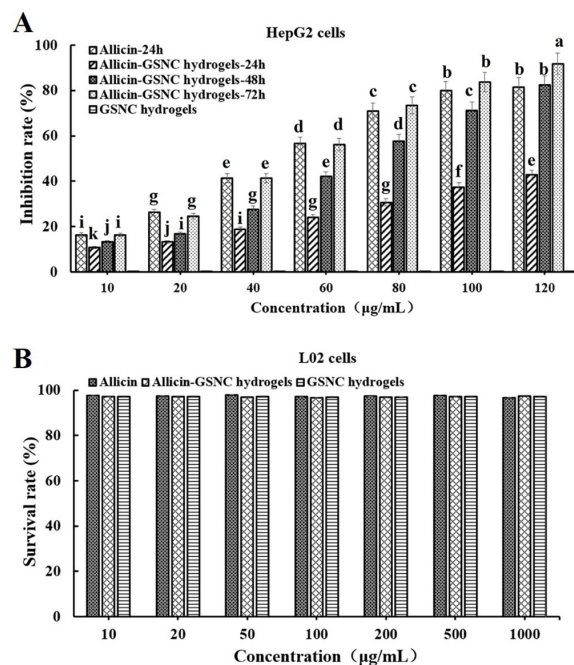


Figure 8. Cytotoxic effects of allicin, Garlic Straw Nanocellulose (GSNC) hydrogels and allicin-GSNC hydrogels against HepG2 cells (A) and L02 cells (B). Data are expressed as mean \pm SD (n = 3). Different letters indicate significant differences between groups ($P < 0.05$).

preliminary confirmed that the surface-modified nanocellulose hydrogels is an ideal carrier in the target release system.

4 Conclusion

In this study, GSC were extracted from garlic stalks, and GSNC hydrogels were synthesized to be used as a drug delivery carrier. The structure of GSC, GSNC and GSNC hydrogels were characterized using FTIR, XRD and SEM analysis. The morphology of hydrogels showed that the hydrogels had a porous structure, which was beneficial to water absorption and drug loading. Then the bioactive compound from garlic, allicin was loaded into GSNC hydrogels. The results revealed that GSNC hydrogels could release allicin slowly and have pH sensitivity. Moreover, allicin-GSNC hydrogels had the highest release rate of allicin in simulated intestinal fluid, and also had a better release rate in simulated tumor growth environment (pH 5.5). In cell-culture study, allicin-GSNC hydrogels significantly showed selective cytotoxicity in HepG2 cell proliferation and non-toxicity in normal hepatocyte cells (L02 cells). Overall the study suggested that allicin-loaded into GSNC hydrogels improved the bioavailability and stability of allicin. GSNC hydrogels have good mechanical properties and has the potential to become a carrier material for drug delivery *in vivo*.

Conflict of interest

No conflict of interest exists in the submission of this manuscript and it is approved by all authors for publication. The original work described here, has not been published previously,

and not under consideration for publication elsewhere, in whole or in part. All the authors listed have approved the manuscript.

Availability of data and material

All data included in this study are available upon request by contact with the corresponding author.

Author contributions

Xudong Gao contributed to the design of experiments, methodology, verification, software, formal analysis and draft the manuscript; Yanan Jia contributed substantially in the cell culture and cytotoxicity assay, data acquisition, statistical analysis, and data interpretation; Zhongqin Chen contributed in the characterization of hydrogels; Ramesh Kumar Santhanam contributed in designing the experiments and check the grammar of the manuscript; Min Zhang contributed mainly in the instrument and software analysis; Chengwei He contributed in the drug release assay *in vitro* and data analysis; Haxia Chen made an important contribution in the conduction and supervision of the experiments, overall manuscript and funding acquisition. All authors read and approved the final manuscript.

Acknowledgements

This work was supported by the grant from the National Key Research and Development Program of China (Grant No. 2021YFE0110000) and Tianjin Municipal Science and Technology Foundation (Grant No. 18PTZWHZ00190).

References

- Abidi, N., Cabrales, L., & Haigler, C. H. (2014). Changes in the cell wall and cellulose content of developing cotton fibers investigated by FTIR spectroscopy. *Carbohydrate Polymers*, 100(2), 9-16. <http://dx.doi.org/10.1016/j.carbpol.2013.01.074>. PMID:24188832.
- Anirudhan, T. S., & Rejeena, S. R. (2014). Poly(acrylic acid-co-acrylamide-co-2-acrylamido-2-methyl-1-propanesulfonic acid)-grafted nanocellulose/poly(vinyl alcohol) composite for the *in vitro* gastrointestinal release of amoxicillin. *Journal of Applied Polymer Science*, 131(17), 8657-8668. <http://dx.doi.org/10.1002/app.40699>.
- Arslaner, A. (2020). The effects of adding garlic (*Allium sativum* L.) on the volatile composition and quality properties of yogurt. *Food Science and Technology*, 40(suppl. 2), 582-591. <http://dx.doi.org/10.1590/fst.31019>.
- Batiha, G.E.-S., Alkazmi, L. M., Wasef, L. G., Beshbishy, A. M., Nadwa, E. H., & Rashwan, E. K. (2020). *Syzygium aromaticum* L. (Myrtaceae): traditional uses, bioactive chemical constituents, pharmacological and toxicological activities. *Biomolecules*, 10(2), 202. PMID:32019140.
- Cheng, X., Cai, W., Chen, X., Shi, Z., & Li, J. (2019). Preparation of graphene oxide/poly(vinyl alcohol) composite membrane and pervaporation performance for ethanol dehydration. *RSC Advances*, 9(27), 15457-15465. <http://dx.doi.org/10.1039/C9RA01379B>. PMID:35514811.
- Dai, H., & Huang, H. (2016). Modified pineapple peel cellulose hydrogels embedded with sepia ink for effective removal of methylene blue. *Carbohydrate Polymers*, 148, 1-10. <http://dx.doi.org/10.1016/j.carbpol.2016.04.040>. PMID:27185109.
- Dai, H., Zhang, H., Ma, L., Zhou, H., Yu, Y., Guo, T., Zhang, Y., & Huang, H. (2019a). Green pH/magnetic sensitive hydrogels based on pineapple peel cellulose and polyvinyl alcohol: synthesis, characterization and naringin prolonged release. *Carbohydrate Polymers*, 209(381), 51-61. <http://dx.doi.org/10.1016/j.carbpol.2019.01.014>. PMID:30732825.
- Dai, L., Cheng, T., Duan, C., Zhao, W., Zhang, W., Zou, X., Aspler, J., & Ni, Y. (2019b). 3D printing using plant-derived cellulose and its derivatives: a review. *Carbohydrate Polymers*, 203, 71-86. <http://dx.doi.org/10.1016/j.carbpol.2018.09.027>. PMID:30318237.
- Dias, O. A. T., Konar, S., Pakharenko, V., Graziano, A., Leão, A. L., Tjong, J., Jaffer, S., & Sain, M. (2021). Regioselective protection and deprotection of nanocellulose molecular design architecture: robust platform for multifunctional applications. *Biomacromolecules*, 22(12), 4980-4987. <http://dx.doi.org/10.1021/acs.biomac.1c00909>. PMID:34791880.
- Eftaiha, A. F., Qinna, N., Rashid, I. S., Remawi, M. M., Shami, M. R., Arafat, T. A., & Badwan, A. A. (2010). Bioadhesive controlled metronidazole release matrix based on chitosan and xanthan gum. *Marine Drugs*, 8(5), 1716-1730. <http://dx.doi.org/10.3390/md8051716>. PMID:20559494.
- Fattahpour, S., Shamanian, M., Tavakoli, N., Fathi, M., Sadeghi-aliabadi, H., Sheykhi, S. R., Fesharaki, M., & Fattahpour, S. (2020). An injectable carboxymethyl chitosan-methylcellulose-pluronic hydrogel for the encapsulation of meloxicam loaded nanoparticles. *International Journal of Biological Macromolecules*, 151, 220-229. <http://dx.doi.org/10.1016/j.ijbiomac.2020.02.002>. PMID:32027902.
- Fufa, B. K. (2019). Anti-bacterial and anti-fungal properties of garlic extract (*Allium sativum*): a review. *Microbiology Research Journal International*, 28, 1-5. <http://dx.doi.org/10.9734/mrji/2019/v28i330133>.
- Gao, X., Chen, Y., Chen, Z., Xue, Z., Jia, Y., Guo, Q., Ma, Q., Zhang, M., & Chen, H. (2019a). Identification and antimicrobial activity evaluation of three peptides from laba garlic and the related mechanism. *Food & Function*, 10(8), 4486-4496. <http://dx.doi.org/10.1039/C9FO00236G>. PMID:31241636.
- Gao, X., Wang, C., Chen, Z., Chen, Y., Santhanam, R. K., Xue, Z., Ma, Q., Guo, Q., Liu, W., Zhang, M., & Chen, H. (2019b). Effects of N-trans-feruloyltyramine isolated from laba garlic on antioxidant, cytotoxic activities and H₂O₂-induced oxidative damage in HepG2 and L02 cells. *Food and Chemical Toxicology*, 130, 130-141. <http://dx.doi.org/10.1016/j.fct.2019.05.021>. PMID:31103739.
- Ge, W., Cao, S., Shen, F., Wang, Y., Ren, J., & Wang, X. (2019). Rapid self-healing, stretchable, moldable, antioxidant and antibacterial tannic acid-cellulose nanofibril composite hydrogels. *Carbohydrate Polymers*, 224, 115147. <http://dx.doi.org/10.1016/j.carbpol.2019.115147>. PMID:31472826.
- Gharekhani, H., Olad, A., Mirmohseni, A., & Bybordi, A. (2017). Superabsorbent hydrogel made of NaAlg-g-poly(AA-co-AAm) and rice husk ash: synthesis, characterization, and swelling kinetic studies. *Carbohydrate Polymers*, 168, 1-13. <http://dx.doi.org/10.1016/j.carbpol.2017.03.047>. PMID:28457428.
- Hanafy, N.A.N., Leporatti, S., & El-Kemary, M. (2020). Mucoadhesive curcumin crosslinked carboxy methyl cellulose might increase inhibitory efficiency for liver cancer treatment. *Materials Science and Engineering: C*, 116, 111119. <https://doi.org/10.1016/j.msec.2020.111119>.
- He, J., Liang, Y., Shi, M., & Guo, B. (2020). Anti-oxidant electroactive and antibacterial nanofibrous wound dressings based on poly(ϵ -caprolactone)/quaternized chitosan-graft-polyaniline for full-thickness skin wound healing. *Chemical Engineering Journal*, 385, 123464. <http://dx.doi.org/10.1016/j.cej.2019.123464>.
- Hosseinzadeh, S., Hosseinzadeh, H., & Pashaei, S. (2019). Fabrication of nanocellulose loaded poly(AA-co-HEMA) hydrogels for ceftriaxone

- controlled delivery and crystal violet adsorption. *Polymer Composites*, 40(S1), E559-E569. <http://dx.doi.org/10.1002/pc.24875>.
- Huang, C., & Shen, X. (2014). Janus molecularly imprinted polymer particles. *Chemical Communications*, 50(20), 2646-2649. <http://dx.doi.org/10.1039/C3CC49586H>. PMID:24469062.
- Kallel, F., Bettaieb, F., Khiari, R., García, A., Bras, J., & Chaabouni, S. E. (2016). Isolation and structural characterization of cellulose nanocrystals extracted from garlic straw residues. *Industrial Crops and Products*, 87, 287-296. <http://dx.doi.org/10.1016/j.indcrop.2016.04.060>.
- Kamel, R., El-Wakil, N. A., Dufresne, A., & Elkasabgy, N. A. (2020). Nanocellulose: from an agricultural waste to a valuable pharmaceutical ingredient. *International Journal of Biological Macromolecules*, 163, 1579-1590. <http://dx.doi.org/10.1016/j.ijbiomac.2020.07.242>. PMID:32755697.
- Kargazadeh, H., Mariano, M., Huang, J., Lin, N., Ahmad, I., Dufresne, A., & Thomas, S. (2017). Recent developments on nanocellulose reinforced polymer nanocomposites: a review. *Polymer*, 132, 368-393. <http://dx.doi.org/10.1016/j.polymer.2017.09.043>.
- Kim, S. W., Bae, Y. H., & Okano, T. (1992). Hydrogels: swelling, drug loading, and release. *Pharmaceutical Research*, 9(3), 283-290. <http://dx.doi.org/10.1023/A:1015887213431>. PMID:1614957.
- Li, X., Shu, F., He, C., Liu, S., Leksawasdi, N., Wang, Q., Qi, W., Alam, M. A., Yuan, Z., & Gao, Y. (2018). Preparation and investigation of highly selective solid acid catalysts with sodium lignosulfonate for hydrolysis of hemicellulose in corncob. *RSC Advances*, 8(20), 10922-10929. <http://dx.doi.org/10.1039/C7RA13362F>. PMID:35541561.
- Lishianawati, T. U., Yusiati, L. M., & Jamhari (2022). Antioxidant effects of black garlic powder on spent duck meat nugget quality during storage. *Food Science and Technology*, 42, e62220. <http://dx.doi.org/10.1590/fst.62220>.
- Liu, Q., Fu, Q., Du, J., & Liu, X. (2022). Experimental study on the role and mechanism of alliin in ventricular remodeling through PPAR α and PPAR γ signaling pathways. *Food Science and Technology*, 42, e31121. <http://dx.doi.org/10.1590/fst.31121>.
- Lou, C., Tian, X., Deng, H., Wang, Y., & Jiang, X. (2020). Dialdehyde- β -cyclodextrin-crosslinked carboxymethyl chitosan hydrogel for drug release. *Carbohydrate Polymers*, 231, 115678. <http://dx.doi.org/10.1016/j.carbpol.2019.115678>. PMID:31888806.
- Lu, Q., Lu, P. M., Piao, J. H., Xu, X. L., Chen, J., Zhu, L., & Jiang, J. G. (2014). Preparation and physicochemical characteristics of an alliin nanoliposome and its release behavior. *Lebensmittel-Wissenschaft + Technologie*, 57(2), 686-695. <http://dx.doi.org/10.1016/j.lwt.2014.01.044>.
- Melguizo-Rodríguez, L., García-Recio, E., Ruiz, C., Luna-Bertos, E., Illescas-Montes, R., & Costela-Ruiz, V. J. (2022). Biological properties and therapeutic applications of garlic and its components. *Food & Function*, 13(5), 2415-2426. <http://dx.doi.org/10.1039/D1FO03180E>. PMID:35174827.
- Nasef, S., ElNesr, E., Hafez, F., Badawy, N., & Slim, S. (2019). Gamma irradiation induced preparation of gum arabic/poly (vinyl alcohol) copolymer hydrogels for removal of heavy metal ions from wastewater. *Arab Journal of Nuclear Sciences and Applications*, 53(1), 208-221. <http://dx.doi.org/10.21608/ajnsa.2019.15587.1246>.
- Nicu, R., Ciolacu, F., & Ciolacu, D. E. (2021). Advanced functional materials based on nanocellulose for pharmaceutical/medical applications. *Pharmaceutics*, 13(8), 1125. <http://dx.doi.org/10.3390/pharmaceutics13081125>. PMID:34452086.
- Nounou, M. M., El-Khordagui, L. K., Khalafallah, N. A., & Khalil, S. A. (2006). In vitro release of hydrophilic and hydrophobic drugs from liposomal dispersions and gels. *Acta Pharmaceutica*, 56(3), 311-324. PMID:19831280.
- Qi, X., Zhang, M., Su, T., Pan, W., Tong, X., Zeng, Q., Xiong, W., Jiang, N., Qian, Y., Li, Z., He, X., Shen, L., Zhou, Z., & Shen, J. (2020). Biocompatible hydrogels based on food gums with tunable physicochemical properties as scaffolds for cell culture. *Journal of Agricultural and Food Chemistry*, 68(12), 3770-3778. <http://dx.doi.org/10.1021/acs.jafc.9b06120>. PMID:32084311.
- Rosas-González, V. C., Téllez-Bañuelos, M. C., Hernández-Flores, G., Bravo-Cuellar, A., Aguilar-Lemarroy, A., Jave-Suárez, L. F., Haramati, J., Solorzano-Ibarra, F., & Ortiz-Lazareno, P. C. (2020). Differential effects of alliin and alliin on apoptosis and senescence in luminal A and triple-negative breast cancer: Caspase, $\Delta\Psi$ m, and pro-apoptotic gene involvement. *Fundamental & Clinical Pharmacology*, 34(6), 671-686. <https://doi.org/10.1111/fcp.12559>.
- Salehi, B., Zucca, P., Orhan, I. E., Azzini, E., Adetunji, C. O., Mohammed, S. A., Banerjee, S. K., Sharopov, F., Rigano, D., Sharifi-Rad, J., Armstrong, L., Martorell, M., Sureda, A., Martins, N., Selamoğlu, Z., & Ahmad, Z. (2019). Alliin and health: a comprehensive review. *Trends in Food Science & Technology*, 86, 502-516. <http://dx.doi.org/10.1016/j.tifs.2019.03.003>.
- Schultz, C. R., Gruhlke, M. C. H., Slusarenko, A. J., & Bachmann, A. S. (2020). Alliin, a potent new ornithine decarboxylase inhibitor in neuroblastoma cells. *Journal of Natural Products*, 83(8), 2518-2527. <https://doi.org/10.1021/acs.jnatprod.0c00613>.
- Setiyoningrum, F., Priadi, G., Afiati, F., Herlina, N., & Solikhin, A. (2021). Composition of spontaneous black garlic fermentation in a water bath. *Food Science and Technology*, 41(suppl. 2), 557-562. <http://dx.doi.org/10.1590/fst.28720>.
- Shang, A., Cao, S.Y., Xu, X.Y., Gan, R.Y., Tang, G.Y., Corke, H., Mavumengwana, V., & Li, H. B. (2019). Bioactive compounds and biological functions of garlic (*Allium sativum* L.). *Foods*, 8(7), 246. <https://doi.org/10.3390/foods8070246>.
- Soumya, R. S., Sherin, S., Raghu, K. G., & Abraham, A. (2018). Alliin functionalized locust bean gum nanoparticles for improved therapeutic efficacy: an in silico, in vitro and in vivo approach. *International Journal of Biological Macromolecules*, 109, 740-747. <http://dx.doi.org/10.1016/j.ijbiomac.2017.11.065>. PMID:29155156.
- Thakur, V. K., & Thakur, M. K. (2014). Processing and characterization of natural cellulose fibers/thermoset polymer composites. *Carbohydrate Polymers*, 109, 102-117. <http://dx.doi.org/10.1016/j.carbpol.2014.03.039>. PMID:24815407.
- Thakur, V., Guleria, A., Kumar, S., Sharma, S., & Singh, K. (2021). Recent advances in nanocellulose processing, functionalization and applications: a review. *Materials Advances*, 2(6), 1872-1895. <http://dx.doi.org/10.1039/D1MA00049G>.
- Valentim, R. M. B., Andrade, S. M. C., Santos, M. E. M., Santos, A. C., Pereira, V. S., Santos, I. P., Dias, C. G. B. T., & Reis, M. A. L. (2018). Composite based on biphasic calcium phosphate (HA/ β -TCP) and nanocellulose from the açai tegument. *Materials*, 11(11), 2213. <http://dx.doi.org/10.3390/ma11112213>. PMID:30412992.
- Wang, Y., Jia, J., Shao, J., Shu, X., Ren, X., Wu, B., & Yan, Z. (2018). Preservative effects of alliin microcapsules on daily foods. *LWT*, 98, 225-230. <http://dx.doi.org/10.1016/j.lwt.2018.08.043>.
- Xie, Z., Shen, J., Sun, H., Li, J., & Wang, X. (2021). Polymer-based hydrogels with local drug release for cancer immunotherapy. *Biomedicine and Pharmacotherapy*, 137, 111333. <http://dx.doi.org/10.1016/j.biopha.2021.111333>. PMID:33571834.
- Yan, L., Wang, L., Gao, S., Liu, C., Zhang, Z., Ma, A., & Zheng, L. (2020). Celery cellulose hydrogel as carriers for controlled release of short-chain fatty acid by ultrasound. *Food Chemistry*, 309, 125717. <http://dx.doi.org/10.1016/j.foodchem.2019.125717>. PMID:31699559.

Yi, Y., Xie, C., Liu, J., Zheng, Y., Wang, J., & Lu, X. (2021). Self-adhesive hydrogels for tissue engineering. *Journal of Materials Chemistry B*, 9(42), 8739-8767. <http://dx.doi.org/10.1039/D1TB01503F>. PMID:34647120.

Zhang, Y., Yu, T., Peng, L., Sun, Q., Wei, Y., & Han, B. (2020). Advancements in hydrogel-based drug sustained release systems for bone tissue engineering. *Frontiers in Pharmacology*, 11, 622. <http://dx.doi.org/10.3389/fphar.2020.00622>. PMID:32435200.